Performance Limits of a Radio-Inertial Lateral Control System for Automatic Landing

DUNCAN MACKINNON* AND PAUL MADDEN†
The Charles Stark Draper Laboratory, Cambridge, Mass.

Parameter optimization techniques are utilized to explore the performance limits of a set of simplified radio-inertial lateral path guidance systems subject to stochastic gusts, radio measurement noise and a constraint on rms control surface activity. The hybrid systems are shown to have rms lateral path errors less than half those of the pure radio systems for equivalent effector activity. The systematic generation of optimized solutions is shown to be particularly valuable in providing a performance bound for a system, against which the performance of a realizable configuration may be measured.

Nomenclature

p = vector of adjustable parameters
x = n-dimensional state
u = m-dimensional Gaussian white noise
E = expected value operator
F = matrix associated with the linear dynamical system; F is a function of the parameter vector p
G = matrix specifying the coupling between the system and the stochastic disturbance vector u
Q = covariance matrix of the white noise process
$f_{1,2}$ = intermediate state variables
J = performance index
p = roll rate
r = yaw rate
v_p = aircraft path velocity
w_y = weight on covariance of lateral position error
w_δ = weight on covariance of effector activity
y = lateral path error
α = radio angular position error
β = sideslip angle
δ = effector deflection
ν = integrator gain factor
ϕ = roll attitude
ψ = heading angle

Subscripts

a = aileron
b = body
i = inertial
n = noise
r = rudder
s = differential spoiler
y = lateral

Presented as Paper 71-957 at the AIAA Guidance Control and Flight Mechanics Conference, Hempstead, N.Y., August 16–18, 1971, submitted August 18, 1971; revision received April 7, 1972. This research was supported by DOT Contract TSC-91. The authors wish to acknowledge the sponsorship of R. Pawlak, Chief of the Landing Systems Program Branch of the DOT Transportation Systems Center, Cambridge, Mass.

Index categories: Aircraft Landing Dynamics; Air Navigation, Communication, and Traffic Control Systems; Navigation, Control, and Guidance Theory.

* Assistant Director. Presently Chief of Control Technology Division, Research, Development and Demonstration Branch of the UMTA, DOT, Washington, D.C. Member AIAA.

† Staff Scientist. Member AIAA.

Introduction

THE increasing utilization of inertial navigation equipment on transport aircraft, a result of the lower cost and high reliability of new equipment, has created interest in the application of inertial data in flight control systems. Particularly attractive are design concepts which permit utilization of inertial position and velocity information in conventional autopilots with a minimum amount of modification.

The benefits of radio-inertial lateral guidance are currently being investigated in a cooperative DOT/TSC-FAA flight test program. A Litton LTN-51 inertial navigator has been modified to provide runway-referenced position and velocity information. A Minimum Hardware Modification (MHM) philosophy has been used by Lear-Siegler in the design of subsidiary analog components which couple the inertial information to the conventional analog "Autoland" autopilot. The system is simplified compared to previously investigated inertially-aided landing systems[1-3] by eliminating lateral acceleration as a feedback variable and the use of relatively simple procedures to eliminate the inertial measurement bias errors in position and velocity.

The MIT Charles Stark Draper Laboratory has been associated with this program during the initial exploration of MHM design concepts and is currently utilizing the MIT/DL Convair 880 digital simulation to validate the response characteristics of the MHM designs. In addition to this digital simulation effort, it was decided to investigate the performance limits of the MHM design using the parameter optimization techniques described in Ref. 3. As a result, it is possible to define the best possible performance that could be expected from an MHM configuration for a specified level of effector activity. The "best performance" can be compared with the performance achieved by the actual design. Such comparisons are useful in evaluating the experimental program and the necessity for more elaborate future experiments.

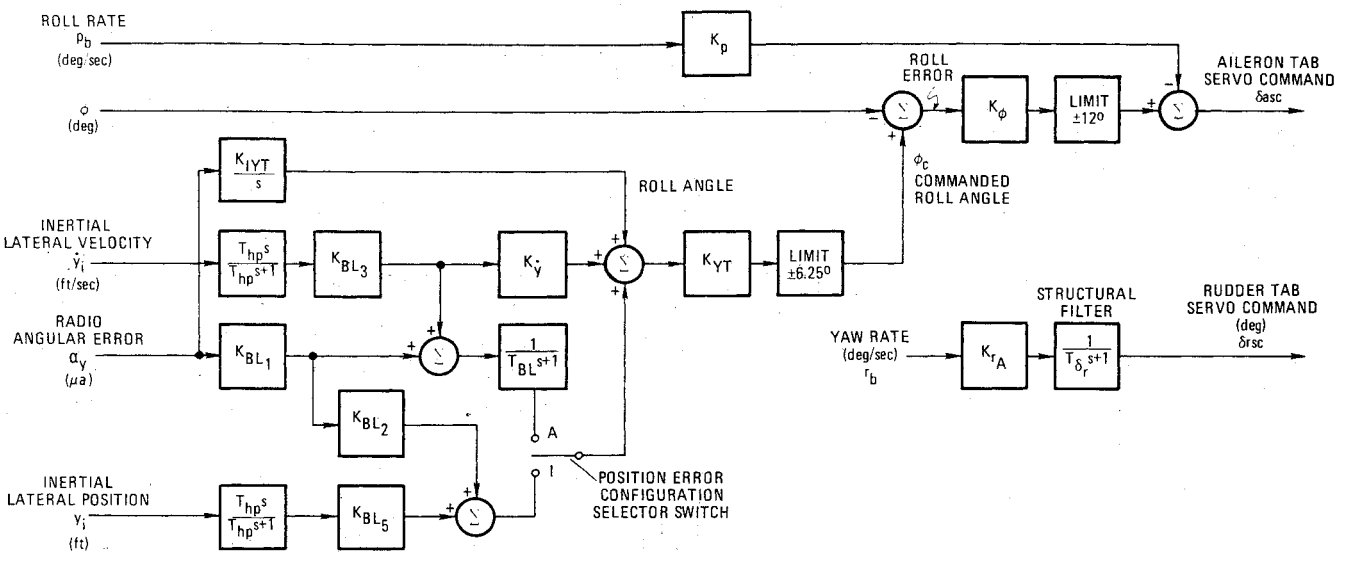

Fig. 1 Minimum Hardware Modification lateral control system with both the 'A' and 'I' configurations shown.

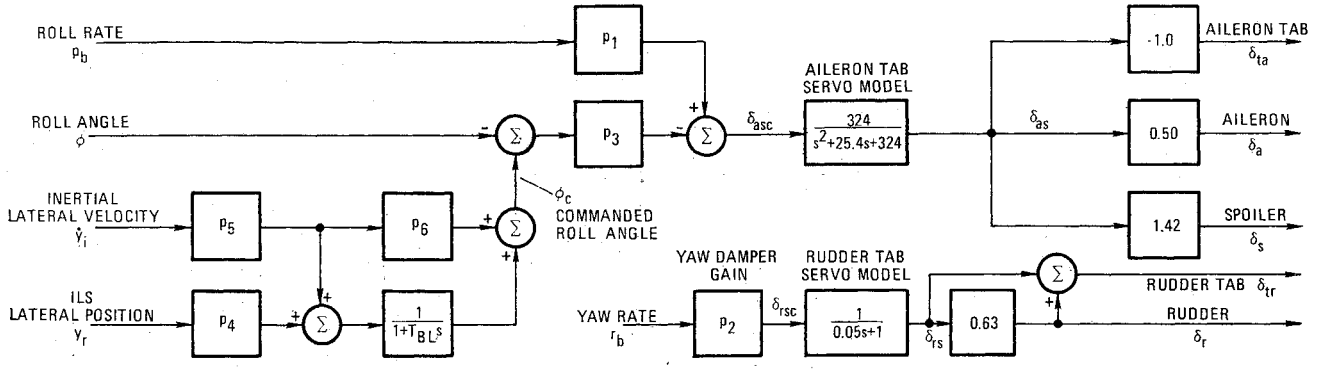

Fig. 2 Simplified model of the 'A' Minimum Hardware Modification lateral control system.

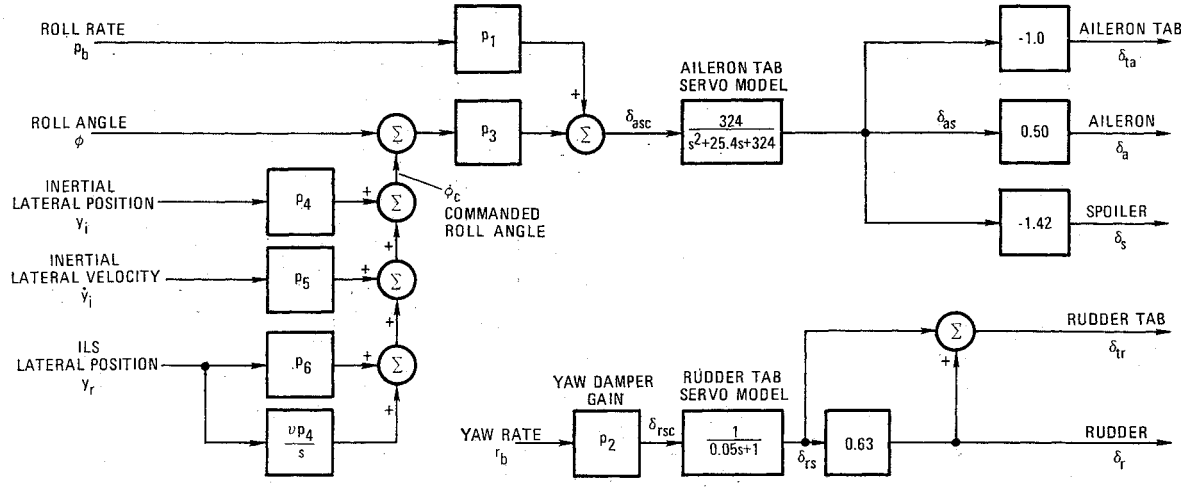

Fig. 3 Simplified model of the 'I' Minimum Hardware Modification lateral control system.

Minimum Hardware Modification Designs

The minimum hardware modification design utilized by Lear is shown in Fig. 1. The control system has two distinct configurations depending on the position of a switch in the position feedback loop, which are identified by the symbols 'A' and 'I'.

Both configurations utilize roll angle, roll rate and lateral inertially-measured velocity for stabilization purposes. The inertial velocity is passed through a lead network with a time constant T_{hp} to eliminate slow variations and bias errors in the velocity signal.

Both systems also utilize integrated angular radio position error to eliminate steady-state errors in position due to wind shear (and inertial position bias errors in the case of the 'I' system).

The 'A' system is identified by its use of radio angular position augmented by filtered inertial velocity for lateral position control. The 'I' configuration, on the other hand, exploits inertial lateral position as well as radio angular position for position reference. The inertial position is passed through a lead network to eliminate slow variations and bias errors. (The same effect is accomplished by the α_y integrator.)

The control system features a 6.25° limit on commanded roll angle to restrict the roll of the vehicle on final approach. A 12° limit is placed on the component of aileron tab deflection arising from the roll error to restrict the magnitude of the roll acceleration.

The lateral control systems feature a yaw rate feedback loop to damp the dutch roll mode. No attempt is made to utilize this system to provide turn coordination. The parameter values associated with the MHM systems are presented in Table 1.

Simplification of the Lateral MHM Control Systems

Exploration of the performance limits of the MHM lateral control systems demands some simplifications to reduce the amount of digital computation time required to yield solutions. The simplified 'A' and 'I' configurations are shown in Fig. 2 and Fig. 3. The simplifications are listed below: 1) The differential spoiler was assumed to be directly proportional to the aileron tab servo output. 2) The hinge moment dynamics between the aileron tab servo output and the ailerons were replaced by a constant gain. 3) The aileron tab servo dynamics were modelled by a second-order linear transfer function. 4) The rudder tab servo in the yaw damper was modelled by a simple time lag, and the structural filter was removed. 5) The rudder hinge moment dynamics were replaced by a constant gain. 6) The lead networks in the inertial position and velocity channels were omitted.

Table 1 Reference parameter values for the 'A' and 'I' MHM configurations

Parameter	Units	Value
K_ϕ	deg/deg	1.280
K_p	deg/deg/sec	0.790
K_{IYT}	sec^{-1}	0.0036
$K_{\dot{y}}$	$\mu a/\mu a$	0.534
K_{YT}	deg/μa	1.000
K_{BL_1}	$\mu a/\mu a$	1.000
K_{BL_2}	$\mu a/\mu a$	0.250
K_{BL_3}	μa/fps	1.500
K_{BL_5}	μa/ft	0.100
T_{BL}	sec	10.000
T_{hp}	sec	65.000

Table 2 Radio measurement noise and environmental disturbance characteristics

Variable	rms noise level	
α_y	0.114	deg
y_r	66.0	ft
β_n	2.0	deg

The utilization of angular error α_y introduces a time-varying gain in the system. In order to eliminate this problem the equivalent position gain was calculated for an aircraft-to-localizer range of 33,000 ft (23,000 ft to the runway threshold). The beam noise superimposed on the radio beam was also calculated for this range. The resulting noise parameters are given in Table 2 along with the rms value of the sideslip angle component due to gusts (corresponding to a 10 fps rms gust velocity). To simplify notation, elements of the parameter vector p were associated with the gains in Fig. 2 and 3.

Optimization Problem Formulation

The technique of stochastic control system design by parameter optimization has been fully described in the literature.[4,5]

Solutions generated by parameter optimization are optimal with respect to a selected performance index. Suppose that it is desired to determine parameters p which minimize the mean square lateral position error, produced as a result of wind gusts and measurement sensor noise, subject to a constraint on mean square aileron-spoiler motion: A performance index reflecting concern with path deviation and effector deflection is

$$J = w_y E(y^2) + w_\delta E(\delta_a{}^2) \tag{1}$$

Systematic parameter optimization techniques were utilized to find a set of parameters p that minimized the performance index, J. The value of w_y was held constant while w_δ was varied to explore a range of solutions.

The lateral vehicle dynamics, control laws, effector servos, and exponentially correlated noise were written in the conventional form of a linear dynamical system

$$\dot{x} = Fx + Gu \tag{2}$$

The state vector and matrices associated with the problem are described by Eqs. (3–6).

$$x = \begin{Bmatrix} \beta \\ p_b \\ r_b \\ \phi \\ y \\ \dot{y} \\ f_1 \\ \delta_a \\ \delta_r \\ f_2 \\ y_n \end{Bmatrix} \tag{3}$$

$$F = \begin{bmatrix}
-0.1485 & 0. & -0.987 & 0.115 & 0. & 0. & 0. & 0.0158 & 0.306 & 0. & 0. \\
-3.73 & -1.52 & 0.8 & 0. & 0. & 0. & 0. & -2.795 & 0.393 & 0. & 0. \\
0.842 & -0.0626 & -0.239 & 0. & 0. & 0. & 0. & -0.127 & -0.4955 & 0. & 0. \\
0. & 1.0 & 0. & 0. & 0. & 0. & 0. & 0. & 0. & 0. & 0. \\
0. & 0. & 0. & 0. & 0. & 1.0 & 0. & 0. & 0. & 0. & 0. \\
-0.72 & 0. & 0.063 & 0.558 & 0. & 0. & 0. & 0.0764 & 0.1487 & 0. & 0. \\
0. & 324.0p_1 & 0. & 324.0p_3 & F_{7,5} & F_{7,6} & -25.8 & -648. & 0. & 324.0p_3 & F_{7,11} \\
0. & 0. & 0. & 0. & 0. & 0. & 0.5 & 0. & 0. & 0. & 0. \\
0. & 0. & 12.6p_2 & 0. & 0. & 0. & 0. & 0. & -20.0 & 0. & 0. \\
0. & 0. & 0. & 0. & F_{10,5} & F_{10,6} & 0. & 0. & 0. & F_{10,10} & F_{10,11} \\
0. & 0. & 0. & 0. & 0. & 0. & 0. & 0. & 0. & 0. & -0.333
\end{bmatrix} \tag{4}$$

'A' Configuration

$F_{7,5} = 0.$ $F_{7,6} = 324.p_3p_5p_6$

$F_{7,11} = 0.$ $F_{10,5} = p_4^2/p_5$

$F_{10,6} = p_4$ $F_{10,10} = -p_4/p_5$

$F_{10,11} = p_4^2/p_5$

'I' Configuration

$F_{7,5} = 324.p_3(p_4+p_6)$ $F_{7,6} = 324.p_3p_5$

$F_{7,11} = 324.p_3p_6$ $F_{10,5} = \upsilon p_4$

$F_{10,6} = 0.$ $F_{10,10} = 0.$

$F_{10,11} = \upsilon p_4$

$$G = \begin{bmatrix}
-0.149 & 0. \\
-3.730 & 0. \\
-0.842 & 0. \\
0. & 0. \\
0. & 0. \\
-0.720 & 0. \\
0. & 0. \\
0. & 0. \\
0. & 0. \\
0. & 0. \\
0. & 0.333
\end{bmatrix} \qquad u = \begin{Bmatrix} u_1 \\ u_2 \end{Bmatrix} \tag{5}$$

Two F matrices are defined corresponding to the MHM 'A' and 'I' systems. The G matrix is the same for both systems. Note that the value of the integrated radio position error in the 'I' system is proportional to the inertial position gain. Thus an increase in p_4 results in a corresponding increase in the integrator gain. In this fashion, the imperfection in the inertial position data is reflected in the optimization process. The integrator gain factor ν can be small if a low drift rate inertial system is used.

The corresponding measurement error in y at a localizer range of 33,000 ft (23,000 ft from the GS antenna) is 66 ft and the sideslip noise component β_n at an approach speed of 280 fps is approximately 2° rms. The Q matrix providing the desired rms values of y_n and β_n is

$$Q = \begin{bmatrix} 10.0 & 0. \\ 0. & 26{,}100. \end{bmatrix} \tag{6}$$

Optimal solutions were generated using the parameter optimization algorithm described in Ref. 4. In essence, an accelerated gradient technique was utilized to produce a sequence of parameter vectors which gradually converged to the optimal solution.

Characteristics of the Optimized 'A' MHM Lateral System

The rms lateral position error of the optimized 'A' system vs rms aileron deflection is plotted in Fig. 4. Since the actual system must include integral compensation to combat windshear, these results are somewhat better than the actual system performance. (The integral compensator was omitted because of XDS 9300 memory capacity limitations.)

Trajectory errors result from noise introduced by ILS beam bends and turbulence. The only source of beam noise is through the ILS lateral position gain p_4. The optimization process responds to this situation by increasing the ILS radio position filter time constant to minimize path deviations due to sensor noise and by increasing the inertial velocity, roll angle and rate gains to minimize gust-induced path errors. This behavior has the undesirable side effect of prolonging the time required to correct initial position errors. The radio position gain and radio position filter time constant were essentially independent of effector activity although the optimization process set them to higher values than the corresponding reference system gains. The variations in the optimal gains as a function of control surface activity are illustrated in Fig. 5. At the reference level of control activity ($\delta_a = 5.2°$ rms), the optimized inertial velocity, roll rate and roll angle gains are essentially identical to the reference system gains; however, the radio position gain and filter time constant are increased by factors of three and fifteen, respectively.

During optimization it was found that the yaw damper gain p_2 had a very small effect on performance; as a result, it converged at a very slow rate. To avoid this problem the value of p_2 was set equal to a constant $p_2 = 20.0$. This value provided an acceptable level of rudder activity of approximately 9° rms.

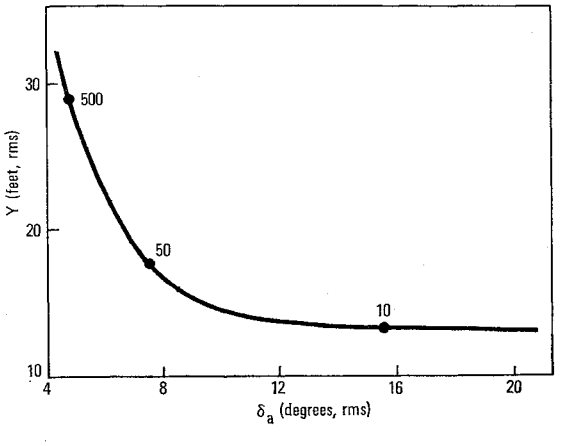

Fig. 4 RMS position error vs rms aileron deflection for the MHM 'A' configuration.

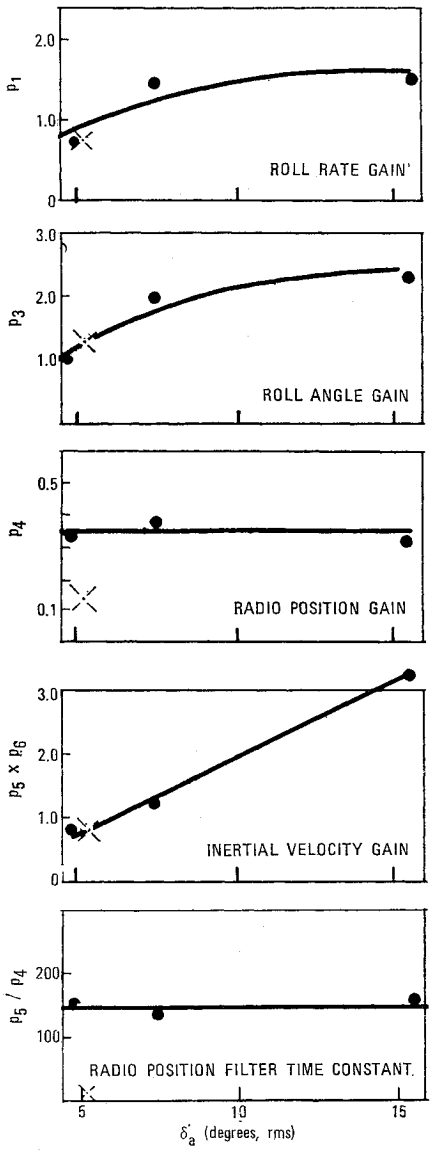

Fig. 5 Parameter values for the reference (X) and the optimized (•) MHM lateral position control systems (configuration 'A').

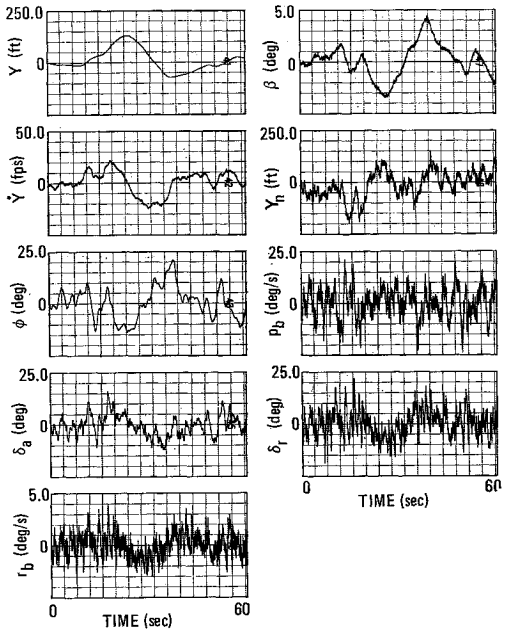

Fig. 6 Response of the reference MHM lateral control 'A' system to aerodynamic and ILS beam noise.

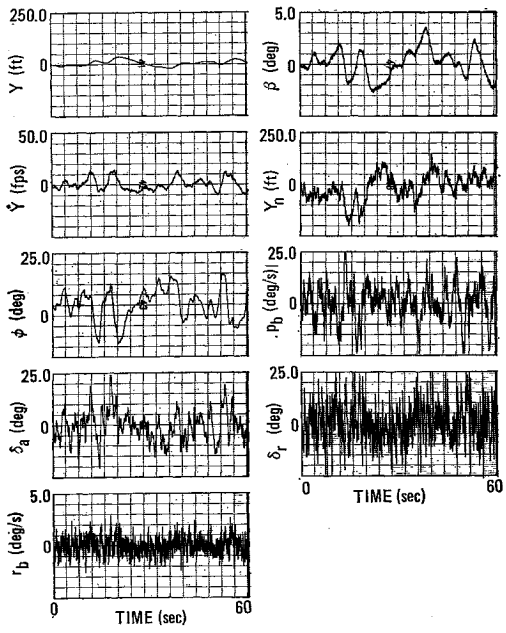

Fig. 7 Response of the optimized MHM lateral control 'A' system ($w_{\delta a} = 50.0$) to aerodynamic and ILS beam noise.

The responses of the reference 'A' system to beam noise and turbulence in Fig. 6 were generated with the linear system and may be compared with those responses (to identical beam noise and turbulence) for the optimized system ($w_{\delta a} = 50$) in Fig. 7. The rms aileron activity for the optimized system (7.4° rms) is only slightly greater than that for the reference system (5.2 rms). The radio noise y_n is, of course, independent of system response. The rms lateral deviation is apparently improved by a factor of about 2.5 validating the analysis.

The transient responses of the reference and optimized configurations are shown in Fig. 8. The optimized system is characterized by a relatively slow (unacceptable) correction of the position error as a result of the increase in radio position filter time constant and lateral velocity feedback gain. The effects of the increases in roll rate, roll angle and inertial velocity gains to combat gusts are apparent in the high-frequency components associated with the roll rate, yaw rate,

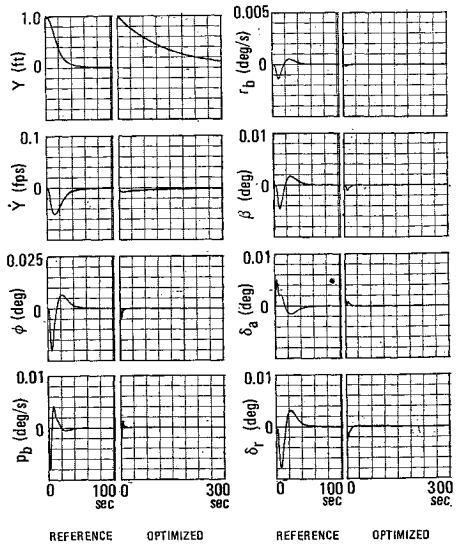

Fig. 8 Response of the reference and optimized MHM lateral control 'A' system to an initial error in lateral position ($w_{\delta a} = 50.0$ for the optimized system).

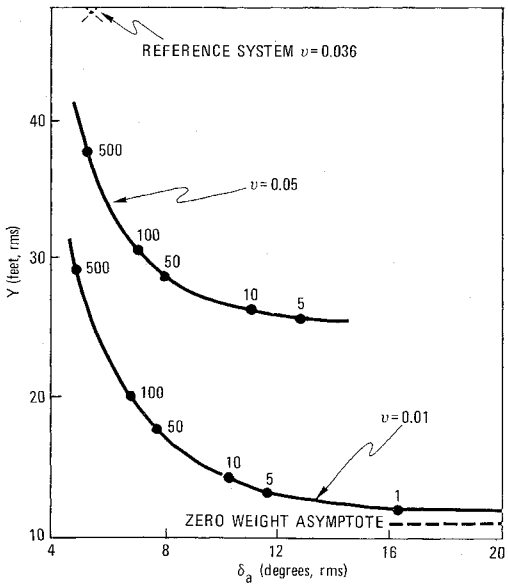

Fig. 9 RMS position error vs rms aileron deflection for the MHM 'I' configuration for two values of ν.

roll angle and effector responses. It will be demonstrated that the undesirable transient response problem associated with the MHM 'A' configuration does not arise in the case of the MHM 'I' configuration.

Characteristics of the Optimized 'I' MHM Lateral System

The 'I' system was optimized for two values of the integral compensator parameter, $\nu = 0.01$ and $\nu = 0.05$. The rms lateral error for the two cases is plotted vs rms aileron deflection in Fig. 9. The effect of increased integral compensator gain is apparent in the greater rms position error for equivalent effector activity. These parametric results provide a quantitative measure of the rms position error degradation associated with increased ability to control the low-frequency position error propagation due to windshear and inertial position measurement bias error.

A source of error is the ILS beam noise introduced through the radio position and integral compensator feedback paths. Since there is an error-free inertial position path available, the optimization process responds by eliminating the direct radio position path ($p_6 \to 0$). In reality, the inertial position will include a low-frequency error (drift) which is inevitably eliminated by the integral compensator, $\nu p_4/s$. An increase in reliance on inertial position (increased p_4) results in a corresponding increase in the integrator gain. Further improvements in trajectory accuracy are obtained by increasing the inertial position and velocity gains together with roll rate and angle gains (p_4, p_5 and p_1, p_3). The variations in the optimal gains as a function of control surface activity are illustrated in Fig. 10. It is seen that the gains for both values of ν vary in an identical manner and have almost identical values except for the integral compensator gain which differs by a factor of approximately five.

At the reference level of control activity ($\delta_a = 5.2°$ rms), the optimized inertial velocity, roll rate and roll angle gains are essentially identical to the reference system gains; however, the inertial position gain is higher by a factor of approximately three.

The responses of the reference 'I' system to beam noise and turbulence were generated with the linear system and may be

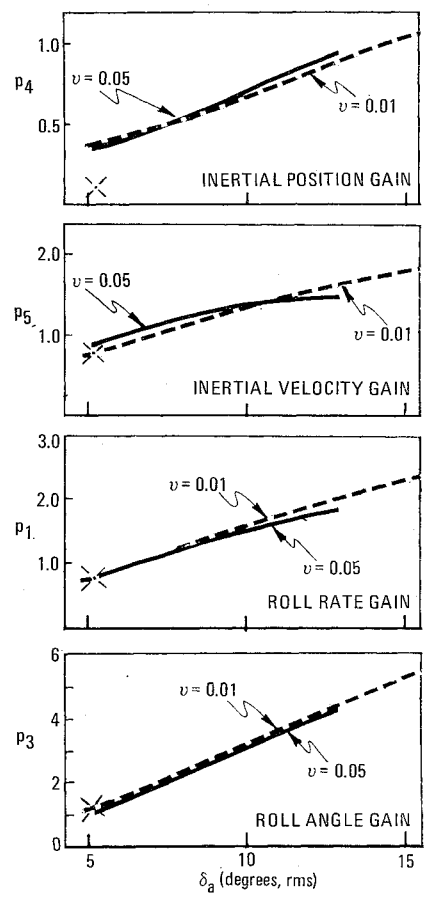

Fig. 10 Parameter values for the reference (X) and the optimized MHM lateral position control systems (configuration 'I').

compared with those responses (to identical beam noise and turbulence) for the optimized system ($\nu = 0.01$, $w_{\delta_a} = 50$) in Fig. 11 and 12. The rms aileron activity for the optimized system (approximately 7.5° rms) is only slightly larger than that for the reference system (5.2° rms). Note that the radio

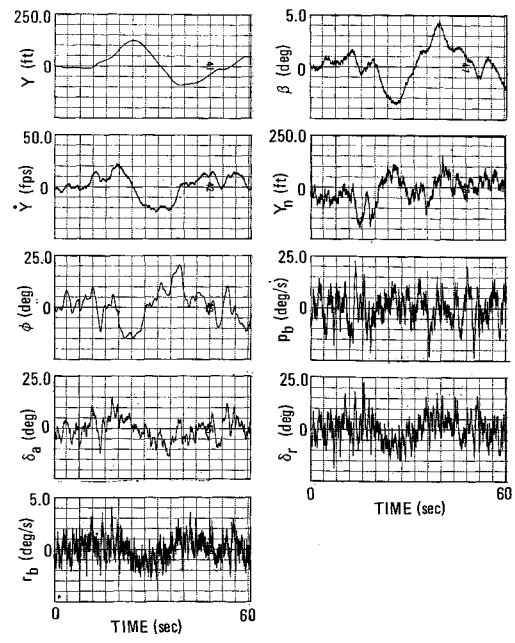

Fig. 11 Response of the reference MHM lateral control 'I' system to aerodynamic and ILS beam noise.

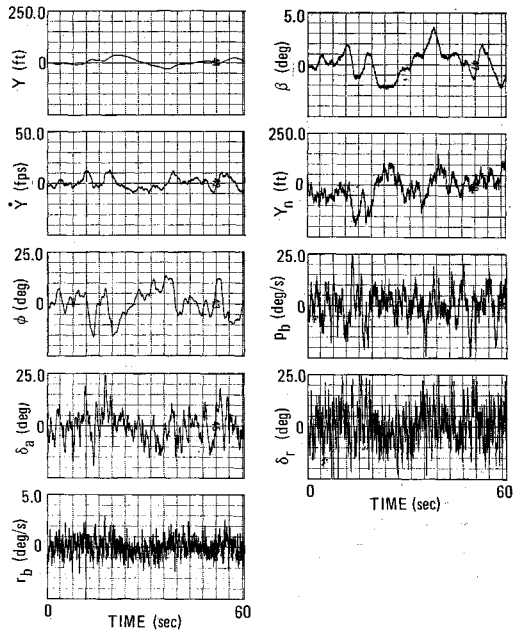

Fig. 12 Response of the optimized MHM lateral control 'I' system ($\nu = 0.01$, $w_{\delta a} = 50.0$) to aerodynamic and ILS beam noise.

noise y_n is independent of the system response. An improvement in rms lateral deviation of approximately 2–2.5 for the optimized system is apparant.

The transient responses of the reference and optimized configurations are shown in Fig. 13. The effect of increased gains is evident in the high-frequency components associated with the optimized responses; however, the lateral position response is fast and well damped compared to that of the optimized 'A' system. Thus the 'I' configuration appears to offer better potential performance than the 'A' system in both the areas of stochastic and transient response.

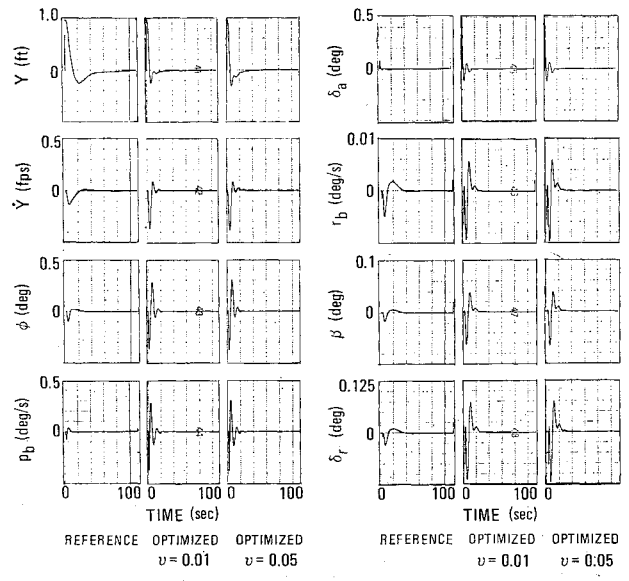

Fig. 13 Response of the reference and optimized MHM lateral control 'I' systems to an initial error in lateral position.

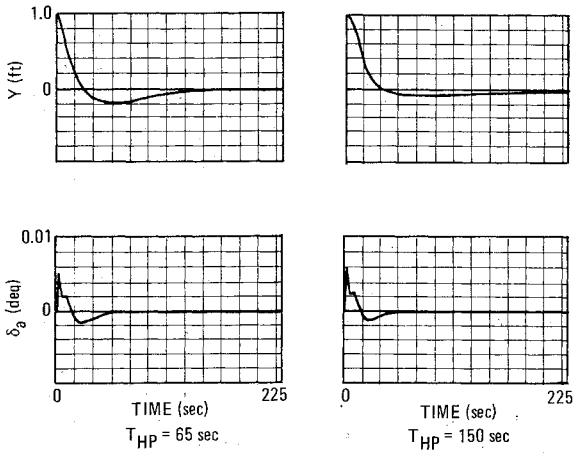

Fig. 14 Effect of the inertial velocity high-pass filter time constant on the reference MHM lateral 'A' system response to an initial error in lateral position (reference gains).

Comparison of the MHM Nonlinear Simulation and the Linear Optimization Models

In order to evaluate the effect of the MHM system/vehicle model simplifications introduced previously, the responses of the full nonlinear CV880 aircraft simulation, including the MHM lateral flight control systems, have been compared with equivalent responses of the linear models used in the optimization studies which incorporated the simplifications tabulated. Figure 14 illustrates the effect of changing the inertial velocity high-pass filter time constant on the MHM lateral 'A' system response. The primary effect is on the low-frequency dynamics as shown by the increase in position response overshoot. Increasing T_{hp} reduces the effect of the high-pass filter. The response of the full-scale simulation (high-pass filters removed) and the simplified linearized models are compared in Fig. 15. Note that the responses are practically identical, justifying the removal of the hinge moment dynamics and other simplifications imposed on the vehicle-effector model.

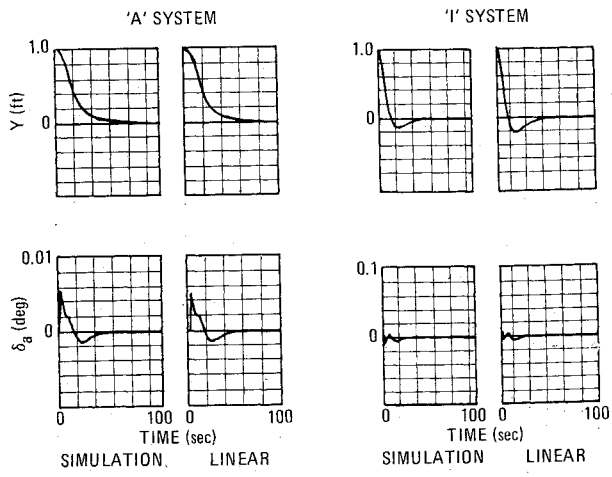

Fig. 15 Comparison of complete nonlinear simulation and simplified linear model responses to an initial error in position with high-pass filters removed from the complete simulation.

Conclusions

The Minimum Hardware Modification (MHM) hybrid radio-inertial couplers achieved substantially lower turbulence and measurement noise-induced rms path errors than the conventional Autoland radio-coupler design. In turbulence of 10 fps (1 sigma), the MHM path errors were less than 50 ft rms compared to 100 ft rms for the conventional design. The reference MHM designs also displayed superior transient response characteristics. An MHM design utilizing inertial position and inertial velocity as feedback variables appears to provide the best combination of transient response characteristics and stochastic performance.

The value of the optimized solutions is seen in providing a performance bound on a system, against which the performance of a realizable configuration may be measured.

References

[1] Multiple Papers, *Conference Proceedings No. 59 on Hybrid Navigation Systems*, NATO AGARD, AGARD-CP-54-69, Sept. 1969.

[2] MacKinnon, D., "Some Applications of Mathematical Optimization Theory to Automatic Landing Systems," R-651, Nov. 1969, MIT Instrumentation Lab., Cambridge, Mass.

[3] Cherry, G., Desai, M., DeWolf, B., Keene, D., MacKinnon, D., and Madden, P., "Space Shuttle Trajectory Management, Guidance, and Control during Approach and Landing," R-662, May 1970, MIT Charles Stark Draper Lab., Cambridge, Mass.

[4] MacKinnon, D. and Madden, P., "Path Accuracy Limitations of Inertially-Based Flight Control Systems in a Turbulent Environment, *Automatica*, Vol. 8, No. 1, Jan. 1972, pp. 23–34.

[5] MacKinnon, D. and Madden, P., "Performance Limits of an Aircraft Inertial-Based Stochastic Lateral Guidance System," *Journal of Aircraft*, Vol. 9, No. 3, March 1972, pp. 217–222.

AUGUST 1972 J. AIRCRAFT VOL. 9, NO. 8,

Automated Aircraft Scheduling Methods in the Near Terminal Area

LEONARD TOBIAS*
NASA Ames Research Center, Moffett Field, Calif.

A general scheduling algorithm for aircraft from terminal area entry to touchdown is developed. The method has the following novel features: 1) Many speed classes of aircraft are considered and speed variations within classes and along portions of the flight path are permitted. 2) Multiple paths are considered which may merge or diverge—the analysis is not restricted to a single runway nor to departures only. 3) Landings are scheduled along conflict free flight paths in minimum time. The algorithm is currently being incorporated in a fast-time simulation of a STOL air traffic system.

Introduction

THIS paper considers the problem of automated scheduling of aircraft in the near terminal area. The need for such scheduling techniques is widely recognized[1]; this is especially true, as Roberts[2] points out, in a commercial STOL environment where we can expect higher traffic density, tighter scheduling and all-weather operations. Previous work has been done in this area for simple situations such as one runway or all aircraft having the same speed; Athans and Porter[3] have presented an optimal control solution for the problem of landing a merging string of vehicles while maintaining adequate separation between aircraft. A computer aided metering and spacing approach to be used with ARTS III can be found in Ref. 4. This paper presents a more general scheduling algorithm in that many speed classes and multiple runways and approach routes are considered. For each aircraft entering the terminal area, the time to landing is minimized; note that this does not obviate the need for priority rules if some over-all objective such as minimum average waiting time/passenger or maximum landing rate is desired. To illustrate this, the effect of mixing speed classes is briefly discussed in the last section.

The terminal area is modeled as a set of nodes of three types: source nodes which represent entry points into the near terminal area; sink nodes which represent the outer markers, and intermediate nodes which represent other key points in the terminal area such as path intersection points and key holding and reporting points. The phrase "entry point" is used here in a more general sense. An entry point or source node can represent not just one point, but a single feeder fix at which many altitude levels are possible. It is assumed, to simplify the discussion, that these alternate paths will merge in the vicinity of the feeder fix and that from the merge point to each outer marker there is a unique nominal air route structure specified. It is further assumed that there is a minimum separation distance d_M that must exist between aircraft and that the en route center has spaced all incoming aircraft by at least this distance. For example, in Fig. 1, the path from entry point S1 to the outer marker O1 is via the intermediate nodes I7, I8, I2, and I3. As seen in Fig. 2, which depicts the vertical flight profile of the nominal air route, I7 is the merge point of the altitude levels. I8 is the point where paths diverge towards each of the runways, I2 is a reporting point prior to the turn onto the base leg. It might be the point at which holding or a delay maneuver is called for

Received January 13, 1972, presented as Paper 72-120 at the AIAA 10th Aerospace Sciences Meeting, San Diego, Calif., January 17–19, 1972; revision received May 1, 1972. The author would like to thank H. Erzberger for many fruitful discussions during the course of this work.

Index category: Air Navigation, Communication, and Traffic Control Systems.

* Research Scientist.